Experimental Cell Research xxx (xxxx) xxx

Contents lists available at ScienceDirect

Experimental Cell Research

journal homepage: www.elsevier.com/locate/yexcr

Pristane promotes anaerobic glycolysis to facilitate proinflammatory activation of macrophages and development of arthritis

Xiaowei Li [a,b,c], Fengjie Gao [a,d], Wenhua Zhu [a,c,*], Congshan Jiang [a,c], Jing Xu [a,c], Jing Zhang [a,b], Liesu Meng [a,b,c,**], Shemin Lu [a,b,c]

[a] Institute of Molecular and Translational Medicine, and Department of Biochemistry and Molecular Biology, School of Basic Medical Sciences, Xi'an Jiaotong University Health Science Center, West Yanta Road No.76, Xi'an, Shaanxi, 710061, China
[b] National & Local Joint Engineering Research Center of Biodiagnostics and Biotherapy, Second Affiliated Hospital, Xi'an Jiaotong University, Xi'an, Shaanxi, 710004, China
[c] Key Laboratory of Environment and Genes Related to Diseases (Xi'an Jiaotong University), Ministry of Education, Xi'an, Shaanxi, China
[d] Yangling Demonstration Zone Hospital, Xianyang, Shaanxi, 712100, China

ARTICLE INFO

Keywords:
Experimental arthritis
Macrophage polarization
Mitochondrial dysregulation
Metabolic reprogramming
Glycolysis

ABSTRACT

Pristane-induced arthritis (PIA) could be adoptively transferred by splenic T cells in rats, and innate immunity should play critical roles in T cell activation. However, in pre-clinical stage, the activation mechanism of innate cells like macrophages remains unclear. Here we found that PIA was dependent on macrophages since cell depletion alleviated disease severity. Splenic macrophages of PIA rats showed M1 phenotypic shifting. The quantitative proteomics analysis suggested that macrophages initiated metabolic reprogramming with the conversion of aerobic oxidation to glycolysis in response to pristane *in vivo*. Notably, macrophages treated with pristane showed mitochondrial dysregulation and increased glycolysis flux and enzyme activity. Additionally, TNFα production, strongly associating with the glycolysis enzyme *Ldha/Ldhb*, could be reduced as glycolysis was inhibited or be enhanced as citrate cycle was blocked. This work provides detailed insights into the molecular mechanisms of pristane-mediated metabolic reprogramming in macrophages and suggests a new therapeutic strategy for arthritic disorders.

1. Introduction

Rheumatoid arthritis (RA) is a common autoimmune disease mainly affecting joints, which heavily imperils the health of patients. The early diagnosis and treatment would alleviate the patients' suffering. Hence lots of researchers devote themselves to the study of RA pathogenesis which is still ambiguous up to now. Macrophages have been proven to participate in the pathogenesis of both RA and experimental arthritis. The increase in the number of macrophages in the synovium was an early hallmark of active rheumatic disease, and high numbers of macrophages were a prominent feature of inflammatory lesions [1]. It was found that macrophages were involved in the pathology of K/BxN serum-induced arthritis [2]. Targeted depletion of macrophages could reduce the severity of arthritis [3]. Immunohistological studies and analysis of dissociated synovium showed that macrophages were the main TNF-producing cells in the inflamed RA joint, and their importance was illustrated by the therapeutic efficacy of TNF blocker in this disease [4]. Macrophages stimulated by excessive interleukin-15 might activate the autoreactive $CD4^+$ T cells in RA [5]. Besides, macrophage-derived reactive oxygen species (ROS) participated in T cell selection, maturation, and differentiation, and also mediated protection against arthritis by suppressing T cell activation [6]. In our previous studies based on pristane-induced arthritis (PIA), an MHC-II restricted and $CD4^+$ T cell-dependent rat model, the increased TLR3 in splenic macrophages played a pivotal role in the initiation and development of arthritis [7,8]. Therefore, the modulation of macrophage activation and function makes much sense for the development of RA and experimental arthritis.

Immunometabolism is a new conception in recent years [9,10].

* Corresponding author. Institute of Molecular and Translational Medicine, and Department of Biochemistry and Molecular Biology, School of Basic Medical Sciences, Xi'an Jiaotong University Health Science Center, West Yanta Road No.76, Xi'an, Shaanxi, 710061, China.
** Corresponding author. Institute of Molecular and Translational Medicine, and Department of Biochemistry and Molecular Biology, School of Basic Medical Sciences, Xi'an Jiaotong University Health Science Center, West Yanta Road No.76, Xi'an, Shaanxi, 710061, China.
E-mail addresses: zhuwenhua@xjtu.edu.cn (W. Zhu), mengliesu@xjtu.edu.cn (L. Meng).

https://doi.org/10.1016/j.yexcr.2020.112404
Received 11 August 2020; Received in revised form 9 November 2020; Accepted 23 November 2020
Available online 24 November 2020

There has been an appreciation that metabolic regulation to immune cells is related to inflammatory diseases [11,12]. For example, Bustos et al. suggested that cytokine production in macrophages was related to the activity of glycolytic enzymes PFK1 and PFK2 [13]. The inflammatory macrophages activated with LPS or the combination of LPS and IFNγ underwent an increase in the metabolism of glucose to lactate together with the decrease of citrate cycle associated oxidative phosphorylation [14–16]. In classically activated (M1) macrophages, glycolytic flux was increased for the production of ROS and ATP and the expression of inflammatory genes. In contrast, oxidative metabolism was better suited to alternatively activated (M2) macrophages, which played anti-inflammatory and tissue repairing roles [17]. As mentioned, different subtypes of macrophages show different metabolic phenotypes, which may be a result of adaption for macrophage function, as well as be a reason leading to the macrophage polarization and activation, indicating the immunometabolism related with macrophages may play an important role in RA and experimental arthritis. However, metabolism and metabolic responses to inflammatory events based on macrophages in the pathogenesis of RA are poorly studied [18,19].

In the present study, we found that M1 macrophages play a significant role in the early stage of PIA. Pristane stimulation to macrophages led to mitochondrial dysfunction and metabolic abnormalities. Splenic macrophages in response to pristane up-regulated glycolysis and down-regulated oxidative phosphorylation to promote the conversion of glucose to lactate. In keeping with this, inhibition of anaerobic glycolysis attenuated pristane-induced TNFα production. Together, our data reveal molecular mechanisms of pristane-mediated macrophage metabolic reprogramming in the development of experimental arthritis and unveil the potential for therapeutic targeting from the perspective of macrophage metabolism for RA.

2. Materials and methods

2.1. Rats and ethical statement

DA rats (originated from Section of Medical Inflammation Research, Karolinska Institutet, Sweden) were maintained under standard specific pathogen-free conditions in the Animal Center of Xi'an Jiaotong University. All rats were maintained in a standard 12 h/12 h light/dark cycle at a constant temperature of 22 ± 2 °C with a relative humidity of 45 ± 10% and provided access to food and water *ad libitum*. The animal experiments were approved by the Institutional Animal Ethics Committee of Xi'an Jiaotong University (No.2018–228).

2.2. Induction and evaluation of arthritis

DA rats at the age of 8–12 weeks were given a single intradermal injection of 150 μL of pristane (2, 6, 10, 14-tetramethylpentadecane; ACROS Organics, USA) at the base of tail to induce PIA, as described previously [20]. Arthritis development and severity were assessed using a macroscopic scoring system as described previously [21].

2.3. Macrophage depletion in vivo

Gadolinium chloride ($GdCl_3$) (1.5 mg/200 g, Sigma) or PBS was administrated *i.v.* to rats one day before arthritis induction. The depletion efficiency was assessed by flow cytometry analysis by detecting $ED1^+$ cells in the blood.

2.4. Cell culture and stimulation

Rat macrophage cell line NR8383 was cultured in F–12K medium (Sigma, USA) containing 15% FBS (HyClone, USA) at 37 °C in a humidified atmosphere of 5% CO_2. The emulsion of pristane with the concentration of 1 mM was made by repeated aspiration with complete medium. For pristane stimulation, 5×10^5 cells per well were plated into a six-well plate overnight, and then the culture medium was replaced with fresh pristane emulsion. In the inhibitor-treated experiment, wortmannin (Sigma, USA) [22], 2-deoxy-D-glucose (2-DG, Sigma, USA) [23], malonic acid (MA, Sigma, USA) and 3-nitropropionic acid (3-NA, Sigma, USA) were applied to NR8383 cells to block autophagy, glycolysis and TCA pathway.

2.5. RNA quantitation

Total RNA from rat splenic macrophages and NR8383 cells was isolated by using TRIzol Reagent (Invitrogen, USA), and cDNA was synthesized by First Strand cDNA Synthesis Kit (Thermo, USA). Realtime quantitative PCR (RT-qPCR) was performed with FastStart Universal SYBR Green Master (Roche, USA) for mRNA quantitation. The relative gene expression normalized by *β-actin* was calculated with $2^{-\Delta\Delta CT}$ method. Primers for *Ldha*, forward: 5′- ACA AGG AGC AGT GGA AGG -3′ and reverse: 5′- GGA CGC TGA GGA AGA CAT -3′. Primers for *Ldhb*, forward: 5′- GAT TCT GCT CGG TTT CGT -3′ and reverse: 5′- GCT GTC ATT GTC CGT TCC -3′. Primers for *Tnfa,* forward: 5′- TCA GCC TCT TCT CAT TCC TGC -3′ and reverse: 5′- TTG GTG GTT TGC TAC GAC GTG -3′. Primers for *Mrc1,* forward: 5′- TCC CTC GGA AAG TGA TGT GC -3′ and reverse: 5′- CCC ATC GCT CCA CTC AAA GT -3′. Primers for *Il1b,* forward: 5′- CTG TGA CTC GTG GGA TGA TGA C -3′ and reverse: 5′- CTT CTT CTT TGG GTA TTG TTT GG -3′. Primers for *Cd163,* forward: 5′- GCA CTG GAA CTG AGG AGC AT -3′ and reverse: 5′- TAC CAA GCG GAG TTG ACC AC -3′. Primers for *β-actin*, forward: 5′- GAG GGA AAT CGT GCG TGA C -3′ and reverse: 5′- GCA TCG GAA CCG CTC ATT -3′.

2.6. Flow cytometry

Flow cytometry was performed on single-cell suspensions from splenic cells and blood. Cells were incubated with Brefeldin A (10 μg/mL, Selleck) for 4 h, followed by a LIVE/DEAD Fixable Dead Cell Stain (Thermo Fisher Scientific, USA), an anti-mouse CD16/CD32 Fc-block (BD Biosciences, USA). For intracellular staining, cells were fixed and permeabilized using BD Cytofix/Cytoperm solution (BD Biosciences, USA). The monoclonal antibodies include ED1-FITC (Bio-Rad, USA), anti-MRC1-Percp-cy5.5 (BIOSS, China) and TNFα-PE (BD Biosciences, USA). Samples were measured by flow cytometry (Guava, Millipore), and the data were analyzed using FlowJo software (TreeStar Inc., USA).

2.7. Splenic macrophage isolation

Splenic macrophages were isolated by Nycodenz (Axis-shield, Norway) and a positive selection with His36 antibody by LS columns (Miltenyi Biotec, Germany). In brief, spleens from DA rat were injected with 2 mL of an enzyme cocktail containing 1 mg/mL collagenase D (Roche, USA), 100 mg/mL DNase I (Sigma, USA) and 0.6 U/mL Dispase (Roche, USA) in DMEM medium. Then the spleen was minced into a homogenous paste by using scissors and incubated the mixture for 30 min at 37 °C in a humidified incubator. Ethylenediaminetetraacetic acid (EDTA) was added to a final concentration of 10 mM and incubated for 10 more minutes. The cell suspension was passed through a 70 μm cell strainer, and cells were resuspended in 2 mL DMEM containing 2 mM EDTA. The cell suspension was carefully added to the top of 5 mL of 14.5% nycodenz solution (nycodenz dissolved in PBS). After spinning at 530×*g* for 20 min without brakes, cells were collected between nycodenz and DMEM (middle layer) and were resuspended in 1 mL PBS. Cells were then incubated with 0.37 mg/mL anti-His36 monoclonal antibody (Santa Cruz Biotechnology, USA) at 4 °C for 15min. After washing twice, 200 μL of anti-mouse lgG MicroBeads (Miltenyi Biotec, Germany) was added to 800 μL cell suspension and incubated at 4 °C for 15 min following the manufacturer's instructions. Finally, His36 positive cells were enriched by LS columns in the magnetic field of a suitable MACS separator (Miltenyi Biotec, Germany) and ensured that at least 5×10^6 positive cells were collected per sample.

2.8. Sample preparation and digestion for mass spectrometry

Cell pellets were resuspended in 300 μL lysis buffer, boiled, sonicated, and the supernatant was extracted after centrifugation at 20,000×*g* for 15 min. The proteins were taken from each group for SDS-PAGE analysis and visualized by Coomassie staining. The concentrations of protein were measured by using the Pierce BCA™ Protein Assay Kit (Thermo Fisher Scientific, USA) and 300 μg of protein was taken in each sample for FASP digestion. Briefly, each sample was added dithiothreitol (DTT) to 100 mM and heated in a boiling water bath for 5 min. After adding 200 μL of urea (UA) buffer (8 M Urea, 150 mM Tris-HCl, pH8.0) and mixing, the samples were transferred to a 10 KD ultrafiltration centrifuge tube and centrifuged at 12, 000×*g* for 15min, and the filtrate was discarded (this step was repeated once). Then, the samples were alkylated with 100 μL iodoacetamide (IAA) (50 mM IAA in UA), shook at 600 rpm for 1 min, and centrifuged at 12,000×*g* for 10 min after 30 min at room temperature in darkness. Another 100 μL UA buffer was added and centrifuged at 12,000×*g* for 10 min (this step was repeated twice). Subsequently, 100 μL NH_4HCO_3 (Sigma, USA) buffer (100 mM) was added to each sample and followed by centrifugation at 14,000×*g* for 10 min (this step was repeated twice). After adding 40 μL Trypsin buffer (6 μg Trypsin in 40 μL NH_4HCO_3 buffer) to each sample and shaking at 600 rpm for 1min, the samples incubated at 37 °C for 16–18 h. The filtrate was collected following by centrifugation at 12,000×*g* for 10 min. After adding an appropriate amount of 0.1% trifluoroacetic acid (TFA) solution, we used C18 cartridge (Thermo scientific EASY column, 75 μm × 120 mm) for desalting, followed by freeze-drying in vacuum. Finally, the peptide was reconstituted with 0.1% formic acid and analyzed LC-MS/MS.

2.9. LC-MS/MS analysis and database search

A proper amount of peptide from each sample was performed on Easy-nLC 1200 chromatography system (Thermo Scientific) for chromatographic separation. The mobile phase consisted water containing 0.1% (v/v) FA (buffer A) and 85% acetonitrile containing 0.1% (v/v) FA (buffer B). Samples were injected on the trap column (100 μm × 20 mm, 5 μm, C18, Dr. Maisch GmbH) and separated on the chromatographic analysis column (75 μm × 150 mm, 3 μm, C18, Dr. Maisch GmbH) with a flow rate of 300 nL/min. The relevant liquid phase gradient was as follows: 0–2 min, B linear gradient from 5% to 8%; 2–90 min, B linear gradient from 8% to 23%; 90–100 min, B linear gradient from 23% to 40%; 100–108 min, B linear gradient from 40% to 100%; 108–120 min, B linear gradient maintained at 100%. After peptide separation, Q-Exactive HF-X mass spectrometer (Thermo Scientific) was used for DDA (data-dependent acquisition) mass spectrometry. Full MS scans were acquired from *m/z* 300 to *m/z* 1800 at resolution 60,000 at m/z 200, with a target AGC of 3E6 and a maximum injection time of 50 ms. MS/MS scans were acquired in high energy collision dissociation (HCD) mode and resolution of 15,000 @ *m/z* 200, with a target AGC of 1E5 and a maximum injection time of 50 ms.

The splenic macrophages proteome data were analyzed using MaxQuant (version 1.6.0.16). The protein identification against the database Uniport-Rattus norvegicus (Rat)-36135- 20200218 (released in February 2020 and including 36,135 sequences). The search followed an enzymatic cleavage rule of trypsin/P and allowed maximal two missed cleavage sites and a mass tolerance of 20 ppm for fragment ions. The false discovery rate (FDR) for peptide and protein was set to 1%. Razor and unique peptides were used for protein quantification.

2.10. Bioinformatics analysis

Perseus software program (Tyanova, Temu, & Sinitcyn, 2016), R statistical computing software and Microsoft Excel were performed for analyses of bioinformatics data. For differentially expressed proteins (DEPs) between different groups, they need meet the condition of fold change > 1.50 or < 0.67 in expression and *P*-values < 0.05. Besides, one-way analysis of variance (ANOVA) and hierarchical clustering (Euclidean distance) were performed on DEPs between different groups. Gene Ontology (GO) and Kyoto Encyclopedia of Genes and Genomes (KEGG) enrichment analyses were performed using the Fisher's exact test, and FDR correction for multiple testing was also performed. Protein-Protein Interaction (PPI) network of identified DEPs was built by searching against the STRING database with the Cytoscape software program.

2.11. Mitochondrial staining

Mito-Tracker Red (Invitrogen, USA) was used to label mitochondria. NR8383 cells with GFP-LC3 stable expressing [24] were stimulated with 1 mM pristane for 6 h and incubated with MitoTracker Red (100 nM) in culture media for 20 min at 37 °C. Excess dye was washed away with PBS. Then, cells were observed by using a fluorescence microscope (Nikon, Japan).

2.12. Cell metabolite assays

ATP and ADP were detected by Shimadzu high-performance liquid chromatography (HPLC) system, consisting of an SPD-20A pump and an LC-20AT UV detector (Shimadzu Corporation, Kyoto, Japan) as described previously by Mutafova et al. [25,26]. MDA levels were evaluated by a color reaction between MDA and thiobarbituric acid (TBA) according to the manufacturer's MDA kit (Beyotime, China) instructions, and the amounts of MDA were measured by absorption at 553 nm. L-lactate contents of NR8383 cells were determined by using the L-Lactate Assay Kit (Sigma, USA) based on lactate dehydrogenase catalyzed oxidation of lactate, in which the formed NADH reduces a formazan (MTT) reagent. The amounts of L-lactate were measured by absorption at 565 nm.

2.13. Detection of mitochondrial membrane potential and ROS

Mitochondrial membrane potential assay kit with JC-1 (Beyotime, China) was used for monitoring the mitochondrial membrane potential by flow cytometry. JC-1 is a monomer and can emits green fluorescence when the mitochondrial membrane potential is low. In contrast, JC-1 accumulates in the matrix of the mitochondria to form J-aggregates and emits red fluorescence when the mitochondrial membrane potential is high. MitoSOX™ Red (Molecular Probes, USA) was used for mitochondrial ROS levels detection according to the manufacturer's protocol, and the fluorescence intensity was measured by flow cytometry (Guava, Millipore).

2.14. Enzyme activity assay

The LDH activity detection method (pyruvate-to-lactate and lactate-to-pyruvate conversions) is obtained from the literature [27,28]. The enzymatic reaction was carried out with sodium pyruvate and NADH or lactic acid and NAD^+ as substrates, and the enzyme activity of LDH was evaluated by absorbance at 340 nm. Pyruvate kinase can catalyze phosphoenolpyruvate to pyruvate, while coupling ADP and pi to generate ATP. The PK activity can be detected by measuring the content of pyruvate [29]. The enzymatic reactions were carried out in the presence of phosphoenolpyruvate, ADP, $MgCl_2$ and KCl at 37 °C for 30 min. Then, the samples were incubated with 2,4-Dinitrophenylhydrazine (0.5 M) for 20 min at 37 °C. The activity of PK was evaluated by measuring the absorption at 520 nm G6PD and 6GPD can catalyze the glucose-6-phosphate to ribulose-5-phosphate and generate NADPH. G6PD and 6GPD activity were also evaluated by measuring the absorbance at 340 nm (the amount of NADPH) as described in previous literature [30,31].

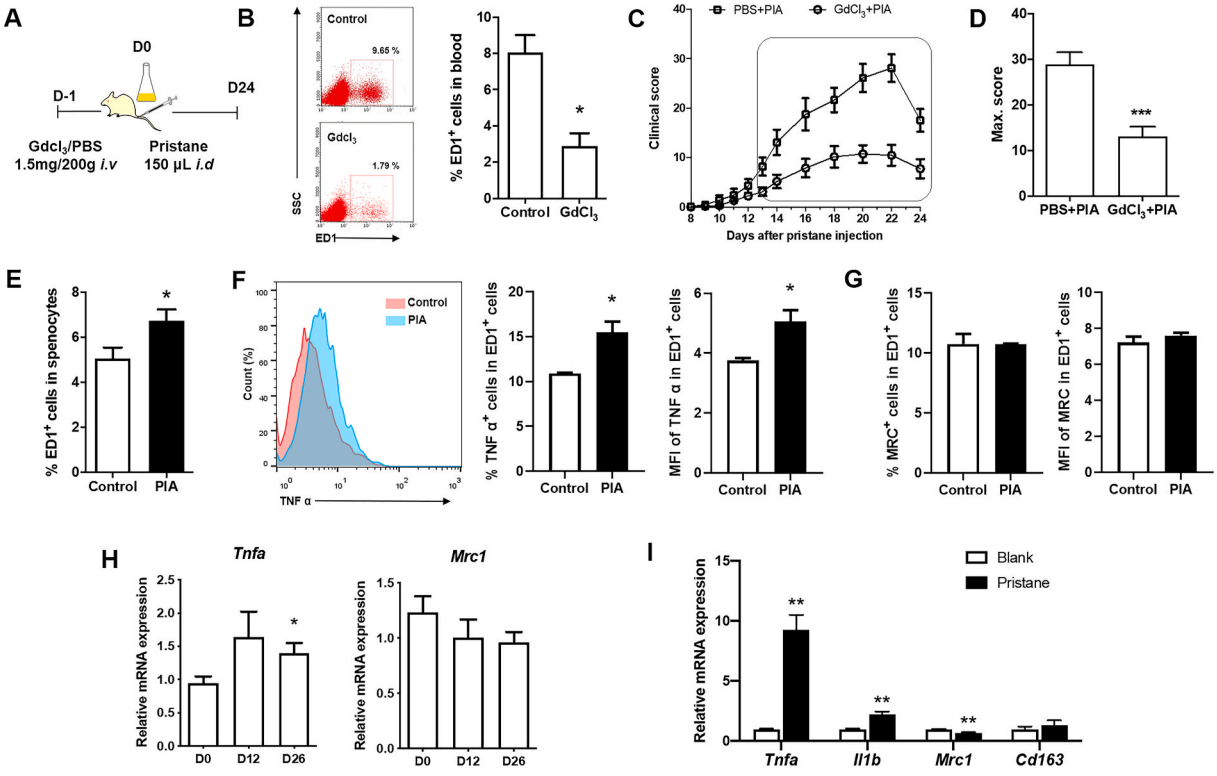

Fig. 1. Pristane treated macrophages, shifting to M1 phenotype, played a critical role in the development of arthritis. (A) Schematic of *in vivo* macrophage depletion and PIA. **(B)** Flow-cytometry-based percentage of ED1$^+$ cells in the blood (n = 3 per group). The arthritis score **(C)** and max score **(D)** of DA-PBS (n = 9) and DA-$GdCl_3$ (n = 14) rats stimulated with pristane. The box represents significance $p < 0.05$. **(E)** Flow-cytometry-based percentage of ED1$^+$ (CD68 antibody, monocytes/macrophages marker in the rat) cells in splenocytes. The percentage and MFI of TNFα$^+$ **(F)** and MRC1$^+$ **(G)** in ED1$^+$ cells on 12th day after pristane injection from PIA and control rats (n = 3 per group). **(H)** *Tnfa* and *Mrc1* mRNA levels of splenic macrophages on day 0 (n = 6), 12 (n = 3) and 26 (n = 3) after pristane injection from DA rats. **(I)** *Tnfα*, *Il1b*, *Mrc1* and *Cd*163 mRNA levels of NR8383 cells with pristane stimulation for 24 h. Data are presented as the mean ± SEM of a representative experiment with three repeats. *$P < 0.05$, **$P < 0.01$, ***$P < 0.001$, Student's *t*-test for two group comparison and one-way ANOVA plus the Bonferroni test for three group comparison.

2.15. LDH isoenzyme assay

Total protein lysates of cells were extracted by RIPA solution (Beyotime, China), followed with incubation on ice for 30 min and centrifugation at 12,000×*g* for 15 min at 4 °C. The final protein concentration of each sample was determined by a BCA kit (Thermo Scientific, USA). 50 μg of protein was loaded onto a 6% (wt/vol) polyacrylamide gel. After electrophoresis, the gel was stained in staining solution containing 0.25 mg/mL nitro blue tetrazolium, 0.03 mg/mL phenazine methosulfate, 5 mM $MgCl_2$, 10 mM NaCl, 0.1 M Tris-HCl (pH 8.6), 1.5 mM NAD$^+$ and 0.1 M sodium lactate [28].

2.16. Statistical analysis

Quantitative data were expressed as mean ± SEM. The statistical analysis of differences between experimental groups was performed using One-way ANOVA or Student's *t*-test. *P* value < 0.05 was considered significant.

3. Results

3.1. M1 macrophages are associated with the development of PIA

The PIA model was established with DA rats by a single *i.d.* injection of pristane, and macrophages of rats were depleted by injecting $GdCl_3$ *i.v.* one day in advance (Fig. 1A). The depletion effect detected by FACS showed that the percentage of ED1$^+$ cells in blood was reduced by 60% on the 3rd day with injection of $GdCl_3$ (Fig. 1B). Rats with pristane injection and macrophage depletion showed alleviated arthritis symptoms and low max arthritis scores compared to control PIA rats, suggesting the critical role of macrophages in arthritis development (Fig. 1C and D).

Macrophage polarization is inseparable from the processes of resolving inflammation. To explore whether pristane affects macrophage polarization, we analyzed the expression of TNFα (M1 marker) and MRC1 (M2 marker) by FACS in splenic macrophages on day 12 with pristane injection. The results showed that the percentage of ED1$^+$ (a rat macrophage marker) cells was significantly higher in DA-PIA splenocytes than that in DA-control splenocytes (Fig. 1E). We further found a significant increase in the percentage and MFI of TNFα$^+$ cells in splenic ED1$^+$ cells, however, there was no difference on percentage and MFI of MRC1$^+$ cells in splenic ED1$^+$ cells (Fig. 1F and G). These results demonstrated that splenic macrophages in PIA rats, shifting to M1 phenotype but not M2, should play a proinflammatory role. Meanwhile, we detected the mRNA expression of *Tnfa* and *Mrc1* in splenic macrophages of DA rats on day 12 and 24 with pristane injection. We found an increase in *Tnfa* expression and a decreased trend in *Mrc1* expression of DA-PIA splenic macrophages compared with control macrophages, which again pointed to the M1 phenotypic shifting (Fig. 1H). Besides, rat macrophage cell line NR8383 was treated with pristane *in vitro* to confirm the finding of macrophage polarization *in vivo*. NR8383 cells also showed a significant increase in *Tnfa*, *Il1b* expression, and a reduction in *Mrc1* expression with pristane stimulation (Fig. 1I). Our results suggested that the splenic macrophages shifting to M1 phenotype might be associated with the development of arthritis.

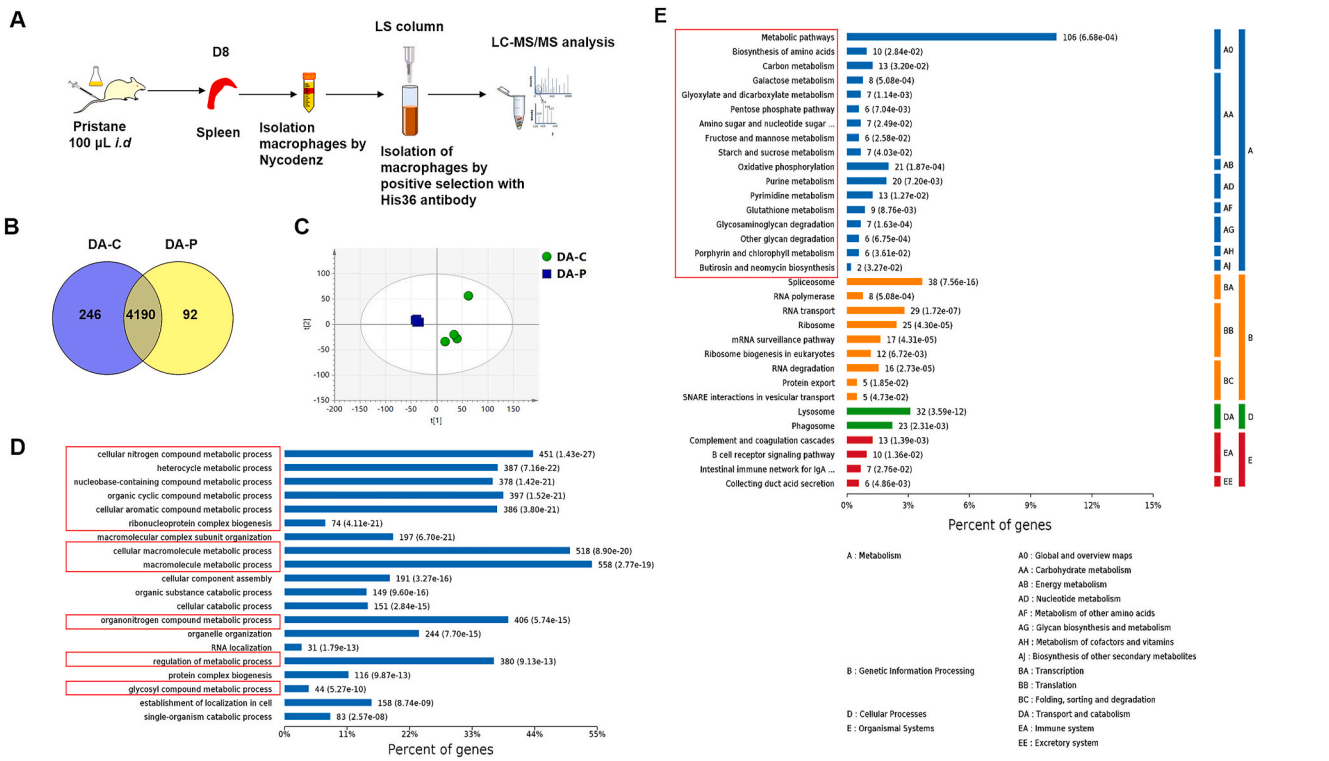

Fig. 2. Quantitative mass spectrometry results and bioinformatic analyses of splenic macrophages in control and PIA rats. (A) Schematic of spleen macrophage isolation from control (DA-C, n = 4) and PIA (DA-P, n = 4) rats and LC-MS/MS analysis. **(B)** Venn diagram for comparison of protein identification results. **(C)** PLS-DA score plots derived from mass spectrometry data for spleen macrophages obtained in DA-C and DA-P groups. **(C)** Venn diagram for comparison of protein identification results. **(D)** GO biological process enrichment analysis. **(E)** KEGG pathway analysis of differential expressed proteins within DA-C and DA-P groups. Data shown are from four rats per group in one single experiment (B–E).

3.2. Functional differences of splenic macrophages between PIA and control rats are revealed by quantitative proteomics

Next, to reveal the potential mechanism whereby pristane regulated macrophage polarization, we performed quantitative mass spectrometry on splenic macrophages of DA rats on day 8 with PBS (DA-C) or pristane (DA-P) injection (Fig. 2A). The Coomassie blue staining of extracted proteins on sodium dodecyl sulfate polyacrylamide gel electrophoresis (SDS-PAGE) showed that the protein quality was acceptable, and there was high parallelism within and between the sample groups (Fig. S1A). A total of 4528 proteins were identified, with all those proteins also being quantitative analyzed with a label-free algorithm (Supplementary Table 1 and Fig. 2B). To visualize the relationship between the different groups of splenic macrophages, a partial least squares discriminant analysis (PLS-DA) was performed within all quantified proteins. The result showed that DA-C and DA-P clearly clustered into two groups (Fig. 2C). A total of 861 differentially expressed proteins (DEPs) (fold change > 1.5 and p-value < 0.05) were found in the of DA-C and DA-P groups (Supplementary Table 2 and Fig. S2B). These data form the basis for quantitative analysis of differences on splenic macrophages between DA-C and DA-P.

To further investigate the functions of these proteins, the analysis of gene ontology (GO), Kyoto encyclopedia of genes and genomes (KEGG) pathways and protein-protein interaction (PPI) networks were performed on DEPs. We showed the enriched top 20 terms of their GO biological process, cellular component and molecular function based on the DEPs between DA-C and DA-P groups. GO biological process analysis revealed that DEPs were mainly distributed in cellular metabolic process, catabolic process, cellular component assembly (Fig. 2D). The top GO cellular component categories that were enriched by DEPs included the intracellular organelle, cytoplasm, extracellular membrane-bounded organelle and intracellular ribonucleoprotein complex (Fig. S1C). The nucleic acid binding, enzyme binding and protein complex binding were the most important terms for the GO molecular function category (Fig. S1D). KEGG pathway enrichment analysis showed that the DEPs of DA-C vs. DA-P were mainly enriched in metabolic pathways, genetic information process, cellular process and organismal systems, of which the metabolic pathway shows the highest significance (Fig. 2E). Further, a PPI network was constructed and displayed associated functions base on the DEPs from the two groups, which presented the significant functions affected by different protein expression patterns (Fig. S1E). Taken together, these results suggested that there were metabolic abnormalities in splenic macrophages after pristane stimulation.

3.3. Metabolism pattern is reprogrammed in pristane stimulated macrophages

To obtain a more detailed metabolic profile of macrophages, we analyzed the protein expression of glycolysis pathway and citrate cycle pathway based on quantitative proteomics data. Heat maps showed an increased trend for the expression of most enzymes in glycolysis pathway after challenge with pristane, and particularly alcohol dehydrogenase (Akr1a1), aldehyde dehydrogenase (Aldh2), hexokinase-3 (Hk3) and ATP-dependent 6-phosphofructokinase (Pfkl) showed a significant increase (Fig. 3A and B). Lactate dehydrogenase (LDH) is one of the most important enzymes in the glycolytic pathway, with two major subunits, LDH-A and LDH-B. LDH-A catalyzes the conversion of pyruvate to lactate and LDH-B is responsible for the conversion of lactate to pyruvate. We found that LDH-A expression did not change, but LDH-B expression was decreased significantly in splenic macrophages of PIA rats (Fig. 3C). Contrary to the results of enzyme expression in the glycolysis pathway, the expression of most enzymes in the oxidative phosphorylation of glucose was decreased, such as dihydrolipoyl dehydrogenase (Dld), pyruvate dehydrogenase (Pdhb) and succinyl-CoA

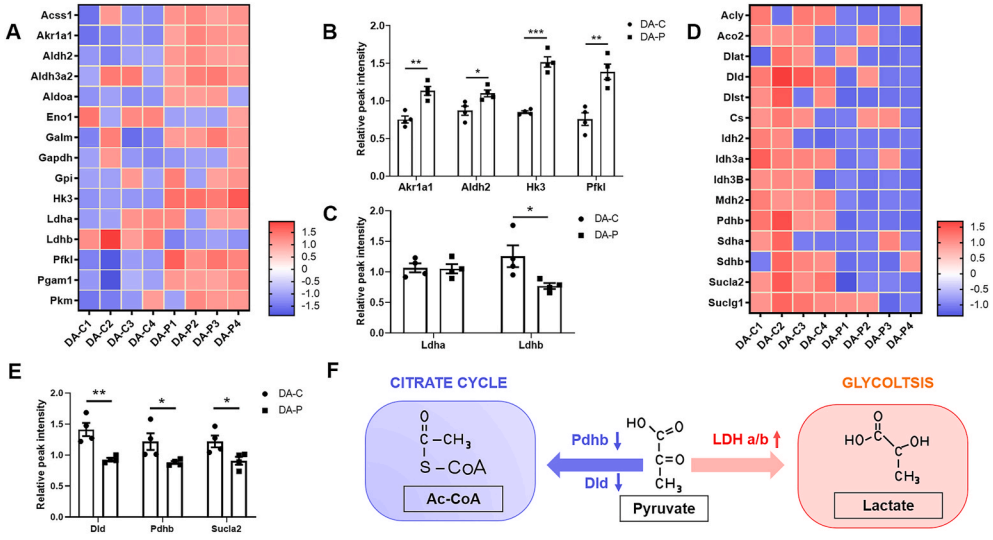

Fig. 3. Pristane induced a switch of aerobic oxidation and anaerobic glycolysis in macrophages in rats. (A) Heat maps showing protein expression of glycolysis/gluconeogenesis pathway. Acss1, acetyl-coenzyme A synthetase; Akr1a1, alcohol dehydrogenase [NADP$^+$]; Aldh2 and Aldh3a2, aldehyde dehydrogenase; Aldh3a2; Aldoa, fructose-bisphosphate aldolase A; Eno1, alpha-enolase; Galm, aldose 1-epimerase; Gapdh, glyceraldehyde-3-phosphate dehydrogenase; Gpi, glucose-6-phosphate isomerase; Hk3, hexokinase-3; Ldha, L-lactate dehydrogenase; Ldhb, L-lactate dehydrogenase B chain; Pfkl, ATP-dependent 6-phosphofructokinase; Pgam1, phosphoglycerate mutase 1; Pkm, pyruvate kinase. **(B, C)** Fold change of Akr1a1, Aldh2, Hk3, Pfkl, Ldha and Ldhb in splenic macrophages of DA-C and DA-P groups (n = 4 per group). **(D)** Heat maps showing protein expression aerobic oxidation (citrate cycle) pathway. Acly, ATP-citrate synthase; Aco2, aconitate hydratase; Dlat, dihydrolipoyllysine-residue acetyltransferase component of pyruvate dehydrogenase complex; Dld, dihydrolipoyl dehydrogenase; Dlst, dihydrolipoyllysine-residue succinyltransferase component of 2-oxoglutarate dehydrogenase complex; Aco2, aconitate hydratase; Cs, citrate synthase; Idh2, isocitrate dehydrogenase [NADP]; Idh3a, isocitrate dehydrogenase [NAD] subunit; Idh3B, isocitrate dehydrogenase [NAD] subunit beta; Mdh2, malate dehydrogenase; Pdhb, pyruvate dehydrogenase E1 component subunit beta; Sdha, succinate dehydrogenase [ubiquinone] flavoprotein subunit; Sdhb, succinate dehydrogenase [ubiquinone] iron-sulfur subunit; Sucla2, succinyl-CoA ligase subunit beta; Suclg1, succinyl-CoA ligase [ADP/GDP-forming] subunit alpha. **(E)** Fold change of Dld, Pdhb and Sucla2 in splenic macrophages of DA-C and DA-P groups (n = 4 per group). **(F)** Regulation of Ac-CoA and lactate production by diverse pathway-related enzymes. Data shown are from four rats per group in one single experiment (A–E). Data are presented as the mean ± SEM. *$P < 0.05$, **$P < 0.01$, ***$P < 0.001$, Student's *t*-test.

ligase subunit beta (Sucla2) (Fig. 3D and E). These data demonstrated that anaerobic glycolysis was enhanced, whereas aerobic oxidation was inhibited in macrophages with pristane treatment (Fig. 3F).

3.4. *Pristane stimulation leads to mitochondrial dysfunction in macrophages*

Since mitochondria are the central place of metabolism, we next detected some indexes of mitochondria in pristane treated NR8383 cell lines. We found that the mitochondrial numbers were reduced in macrophages stimulated with pristane for 6 h by using Mito Tracker Red, whereas LC3-GFP showed aggregation suggesting an induction of autophagy which was consistent with the result of our previous study [24] (Fig. 4A). The mitochondrial membrane potential also was impaired by pristane stimulation, which was detected by JC-1 aggregates/monomers measurement (Fig. 4B). Besides, pristane stimulation induced a high level of mitochondrial ROS and MDA, a lipid peroxidation product (Fig. 4C and D). The loss of membrane potential, overproduction of mitochondrial ROS and MDA suggest that pristane stimulation might damage mitochondria of cells and their function. In addition, the intracellular ATP concentration was decreased, and the ratio of AMP/ATP was increased in cells treated with pristane, which might be an outcome of fewer mitochondria (Fig. 4E). Hence, there was sufficient evidence to believe that the reduction of mitochondria would lead to a unique metabolism pattern in pristane treated macrophages.

3.5. *Pristane treatment results in a metabolic switch to anaerobic glycolysis in macrophages*

Subsequently, we used pristane to simulate NR8383 cell lines *in vitro* to validate the effect on the reprogramming of metabolism. The result clearly showed that the concentration of intracellular L-lactate was significantly increased at 6 h in macrophages with pristane stimulation (Fig. 5A). Moreover, the enzymatic activity of LDH converting pyruvate to lactate was significantly elevated, while that of LDH converting lactate to pyruvate was decreased from 6 h to 48 h in NR8383 cells with

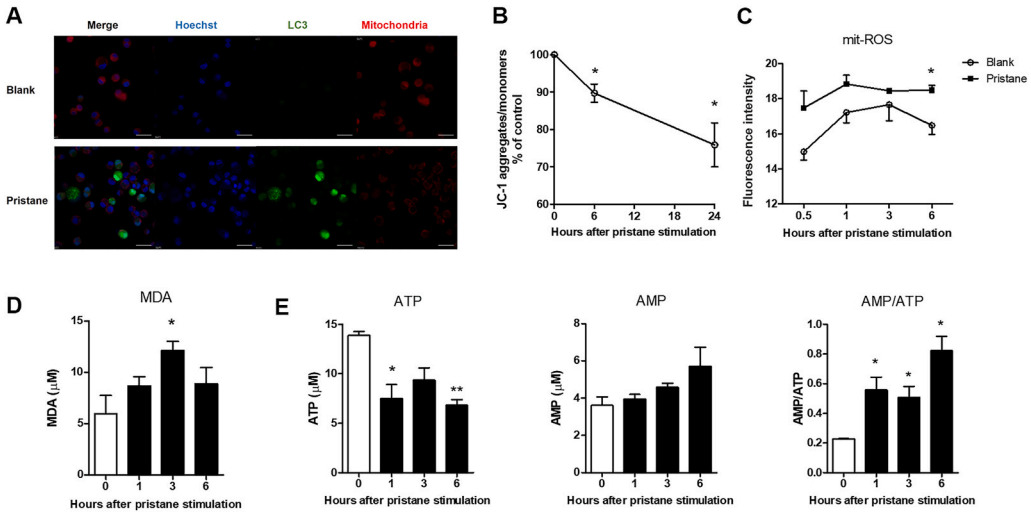

Fig. 4. Macrophages exposed to pristane showed mitochondrial dysfunction. (A) Representative confocal images of LC3-GFP plasmid transfected NR8383 cells stained for mitochondria (Red) and Hoechst at 6 h after pristane stimulation. Images are from one representative experiment of three repeats. Scale bar indicates 20 μm. **(B)** Detection of JC-1 aggregates/monomers in NR8383 cells stimulated with pristane for 6 h (n = 3) and 24 h (n = 3), by flow cytometry. **(C)** The mitochondrial ROS in NR8383 cells simulated with or without pristane for 0.5 h, 1 h, 3 h, 6 h (n = 3 per time point) was stained by MitoSOX and examined by flow cytometry. **(D)** The MDA concentration was detected in NR8383 cells simulated with pristane for 0 h, 1 h, 3 h, 6 h (n = 3 per time point) by lipid peroxidation kit. **(E)** The intracellular AMP and ATP production detected in NR8383 cells simulated with pristane for 0 h, 1 h, 3 h, 6 h (n = 3 per time point) by the HPLC. Data are presented as the mean ± SEM of a representative experiment with three repeats. *$P < 0.05$, **$P < 0.01$, Student's *t*-test for two group comparison and one-way ANOVA plus the Bonferroni test for three group comparison. (For interpretation of the references to color in this figure legend, the reader is referred to the Web version of this article.)

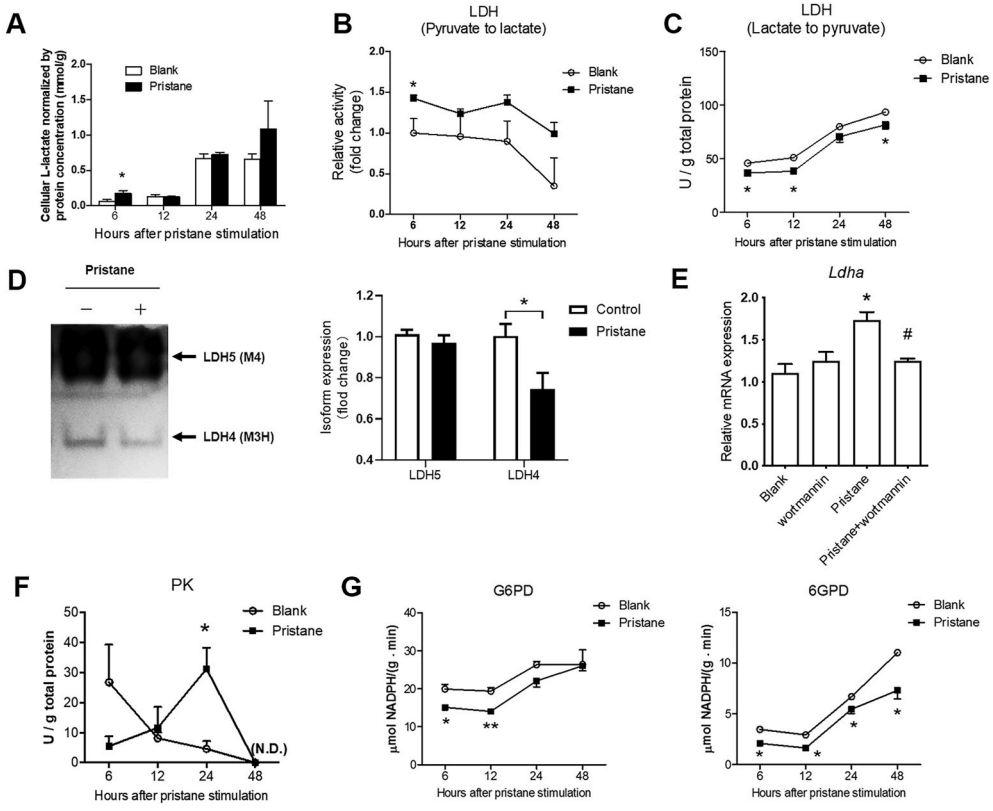

Fig. 5. Pristane treatment in macrophages resulted in the conversion to lactate of glycolysis pathway and reduction of enzyme activity in PPP pathway. (A) L-lactate content normalization by total protein in NR8383 cells with or without pristane treatment for 6 h, 12 h, 24 h, 48 h (n = 3 per time point). Detection of LDH activity: pyruvate-to-lactate **(B)** and lactate-to-pyruvate **(C)** in NR8383 cells with or without pristane treatment (n = 3 per time point). **(D)** LDH isoenzyme composition in NR8383 cells and quantification of the LDH 4 and LDH 5 (n = 3 per group). **(E)** Relative mRNA levels of *Ldha* in NR8383 cells with wortmannin (100 nM) and/or pristane (1 mM) stimulation. # indicated the comparison between pristane group and pristane + wortmannin group (n = 3 per group). **(F)** Pyruvate kinase activity normalized by total protein in NR8383 cells with or without pristane treatment (n = 3 per time point). **(G)** G6PD and 6GPD activity in NR8383 cells with or without pristane treatment (n = 3 per time point) by detecting the amount of NADPH production. Data are presented as the mean ± SEM of one representative experiment from three repeats (F and G). */#$P < 0.05$, **$P < 0.01$, Student's *t*-test for two group comparison and one-way ANOVA plus the Bonferroni test for three group comparison.

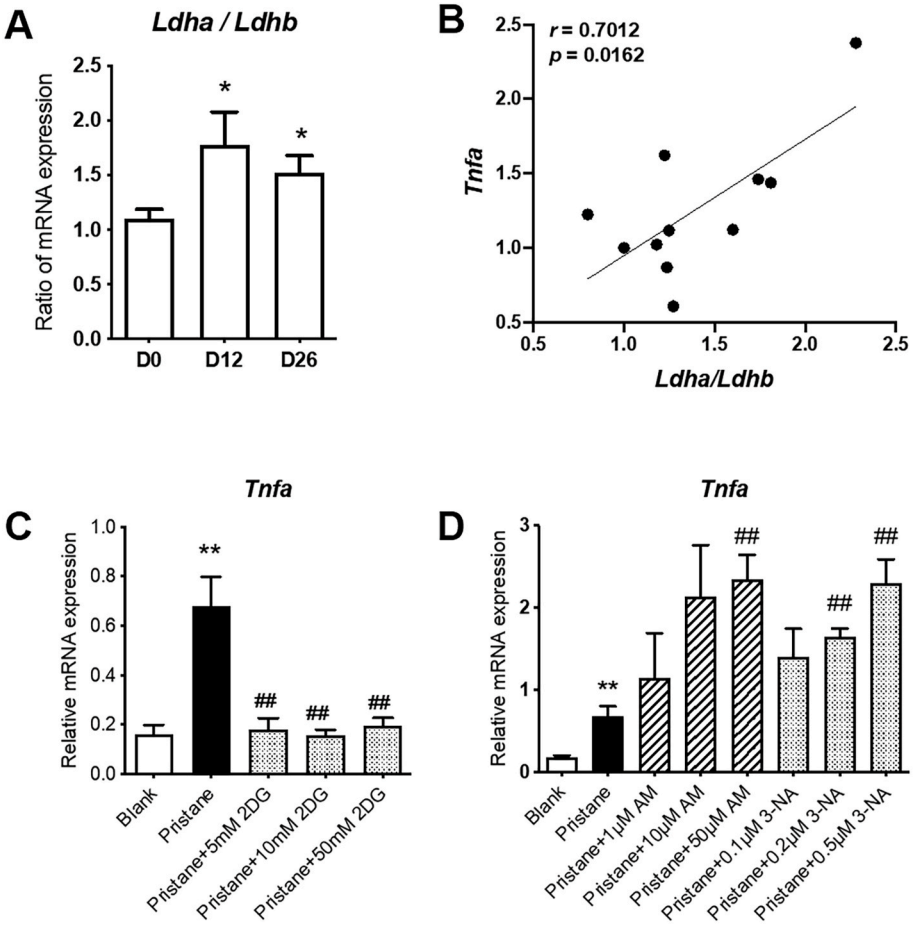

Fig. 6. Pristane-induced glycolysis was required for TNFα production in macrophages. (A) Relative mRNA expression ratio of *Ldha/Ldhb* in splenic macrophages on day 0 (n = 5), day 12 (n = 3) and day 26 (n = 3) after pristane treatment. Data shown represent mean ± SEM of one experiment with two repeats. $^{*}P < 0.05$, one-way ANOVA plus the Bonferroni test. **(B)** Correlation of *Ldha/Ldhb* and *Tnfa* gene expression in splenic macrophages on day 0 (n = 5), day 12 (n = 3) and day 26 (n = 3) after pristane treatment was analyzed by Pearson correlation analysis. **(C)** The mRNA expressions of *Tnfa* in NR8383 stimulated by pristane (1 mM) with 2-DG (5 mM or 10 mM or 50 mM, n = 4 per group) for 24 h. **(D)** The mRNA expressions of *Tnfa* in NR8383 stimulated by pristane (1 mM) with AM (1 μM or 10 μM or 50 μM, n = 3 per group) or 3-NA (0.1 μM or 0.2 μM or 0.5 μM, n = 3 per group) for 24 h * represents the comparison with blank, and # with pristane group. Data are presented as the mean ± SEM of a representative experiment with three repeats. $^{*}P < 0.05$, $^{**/\#\#}P < 0.01$, Student's *t*-test for two group comparison and one-way ANOVA plus the Bonferroni test for three group comparison.

pristane stimulation (Fig. 5B and C). Two subunits, LDH-A and LDH-B of LDH can assemble into five different isoenzyme tetramers, LDH1, LDH2, LDH3, LDH4, and LDH5 [32]. NR8383 macrophages mainly expressed LDH5 (including four LDH-A subunits) and LDH4 (including three LDH-A subunits and one LDH-B subunit). LDH4 is known to catalyze less pyruvate to lactate but more lactate to pyruvate compared with LDH5 due to the LDH-B subunit [28,33]. Hence we performed gel electrophoresis to gain insights into the LDH isoenzyme-type switching in cells stimulated with pristane. After 12 h of pristane stimulation, the protein level of LDH5 did not change, but the protein level of LDH4 was decreased significantly, indicating a lower expression of LDH-B (Fig. 5D). In addition, pristane stimulation to NR8383 cells could increase the mRNA expression of *Ldha* (Fig. 5E). These results clearly showed that pristane treatment led to the LDH isoenzyme conversion with higher capacity to producing lactate. Interestingly, we also found that the increased *Ldha* expression could be blocked by inhibition of autophagy using a PI3K inhibitor wortmannin, which suggested that metabolic regulation might be one of the significant effects of pristane-enhanced autophagy that we previously reported [24] (Fig. 5E).

Pyruvate kinase (PK) as a rate-limiting glycolytic enzyme could provide insights into points of glycolysis regulation, and we further measured its activity by measuring the content of pyruvate. The PK enzyme activity of NR8383 was increased significantly at 24 h with stimulation of pristane (Fig. 5F). On the other hand, the enzymatic activity of glucose-6-phosphate dehydrogenase (G6PD) and 6-phosphogluconate dehydrogenase (6GPD) of pentose phosphate pathway (PPP) was also determined by measuring the amount of NADPH produced, and the results showed that pristane stimulation reduced the enzymatic activity of both G6PD and 6GPD (Fig. 5G). Overall, these results supported that pristane shifted metabolic reprogramming toward anaerobic glycolysis while attenuated citrate cycle pathway and PPP pathway in macrophages.

3.6. Glycolysis promotes M1 phenotype of macrophages with pristane treatment

To further confirm the correlations between glycolysis and macrophage polarization in experimental arthritis, we detected mRNA expression ratio of *Ldha/b* in splenic macrophages of PIA rats. As expected, the ratio of *Ldha/b* showing the level of glycolysis was increased significantly, and also showed a strong correlation with the increased expression of *Tnfa* expression (Fig. 6A and B). To determine whether glycolysis affected the capacity to induce inflammation of macrophages, we stimulated NR8383 cells with pristane in the presence of 2-deoxy-D-glucose (2-DG), an inhibitor of glycolysis. 2-DG with different concentrations all significantly attenuated pristane-induced *Tnfa* expression (Fig. 6C). Given the alterations in citrate cycle metabolism, we also performed NR8383 cells with pristane in the presence of malonic acid (MA) and 3-nitropropionic acid (3-NA), two inhibitors of succinate dehydrogenase in citrate cycle. Contrary to the effect of 2-DG, both MA and 3-NA could elevate the expression of TNFα (Fig. 6D). Altogether these data indicated that pristane enhanced glycolysis facilitated macrophage proinflammatory activation in the progress of arthritis.

4. Discussion

RA is a heterogeneous chronic inflammatory disease, in which distinct clinical phenotypes are thought to develop due to complex interactions between genetic and environmental factors. Experimental

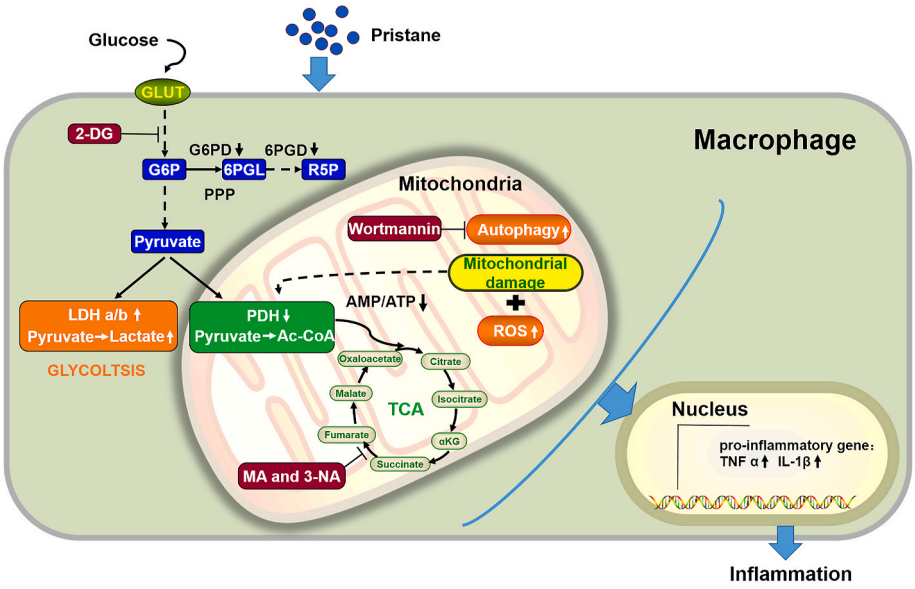

Fig. 7. Graphical summary of pristane-induced metabolic reprogramming in splenic macrophages.

arthritis models are widely used in the studies of RA. PIA is a model established with rats susceptible to arthritis, which has similar symptoms and chronic course as RA [34,35]. In our previous studies, the activation of splenic macrophages through TLR3 pathway could affect the initiation and development of PIA [7]. If the macrophages were depleted with $GdCl_3$, which is known to transiently deplete liver Kupffer cells and spleen macrophages after intravenous administration [36], arthritis severity was significantly decreased suggesting that macrophages should play an important role in PIA pathogenesis, and the function of macrophages in PIA should be explored further.

The activated macrophages are classified into different subtypes, such as M1 and M2 (including M2a, M2b, M2c and M2r), according to the source of macrophages, the definition of activators, and a consensus collection of markers [37,38]. It had arrived at a partial consensus to describe the broad grouping of macrophage activation phenotypes. M1 cells, classically activated macrophages, have proinflammatory effector functions, while M2 cells, alternatively activated macrophages, have anti-inflammatory properties [39]. In the present study, the splenic macrophage showed M1 but not M2 characteristics during the PIA development. The rat macrophage cell line, NR8383, was stimulated with pristane also displayed M1 profile. Hence, we believed that pristane could induce M1 polarization *in vivo* and *in vitro*, and M1 macrophages should play a key role in PIA pathogenesis. However, the mechanism of how pristane induces M1 is still missing.

Recently, the metabolomic studies show that RA is associated with metabolic disruption [18]. Previous studies found that glucose metabolism plays a pivotal role in the pathogenesis of RA, and the synovial tissue in patients with RA showed an increased glycolytic enzyme activity [40]. It had been confirmed that the key enzyme of glycolysis, such as glucose phosphate isomerase (GPI) [41], triose phosphate isomerase (TPI) [42] and PK [40] could take part in the occurrence and development of RA. Our quantitative proteomics data confirmed that most of the DEPs were associated with metabolic process in pristane treated macrophages. We have gone on to show that pristane trigger a switch away from aerobic oxidation toward anaerobic glycolysis, with important functional effects.

Mitochondria play a significant role in energy metabolism, including integrating various metabolic pathways, regulating apoptosis, maintaining Ca^{2+} homeostasis, and producing physiological levels of ROS [43]. Here we found that ROS production in mitochondria, MDA concentration and the ratio of AMP/ATP was increased, and mitochondria numbers and ATP levels was decreased in pristane treated macrophages, suggesting that mitochondria was impaired and dysregulated, which might relate to the changes in mitochondrial metabolism. In our previous study, it was found pristane could induce autophagy in macrophages treated with pristane [24], which might be the reason for mitochondria dysfunction that we have observed in the present research. In several studies, it has been observed in reductions of mitochondrial membrane potential, perinuclear clustering of mitochondria and autophagosome formation in fibroblast-like synoviocytes (FLS) from patients with RA [44,45]. In a complementary study comparing RA and OA, it was found that FLS from patients with RA had a higher ratio of glycolysis rate to respiration rate, which implied that FLS of RA patients tended to the energy obtained by glycolysis [45]. By studying macrophages stimulated by pristane, we confirmed that pristane could also change the function of mitochondria, which might lead to metabolic disruption of macrophages in PIA model.

In recent years, immunometabolism is considered as a governor and controller for macrophage function [46,47]. It governs the phenotype of immune cells by controlling transcriptional and posttranscriptional events rather than is the adaptive outcome of different functions. More recent studies have confirmed that a shift toward glycolysis and fatty acid synthesis, and away from Krebs cycle and fatty acid oxidation, make macrophages pro-inflammatory [17,48]. Therefore, different metabolism pathways of glucose were assessed further. The enzymatic activity of LDH converting pyruvate to lactate, as well as PK, was promoted in pristane treated macrophages, while the PPP pathway was inhibited. These changes in enzyme activity might be responsible for the increase of cellular lactate concentration in macrophages stimulated with pristane. Another interesting thing was, if the autophagy was blocked with wortmannin, the mRNA expression of *Ldha* would be suppressed, which indicates that anaerobic glycolysis might be initiated by autophagy induced by pristane.

Because two subunits of LDH, LDH-A and LDH-B are responsible for the opposite reaction direction between lactate and pyruvate separately, the ratio of LDH-A/B would indicate the main reaction direction in the cells [49]. In the present results, the ratio of *Ldha/b* mRNA was elevated in the splenic macrophages of PIA rats, indicating that anaerobic glycolysis was enhanced in the cells. Furthermore, this ratio correlated with TNFα, a marker of M1, which was another evidence that anaerobic glycolysis related to macrophage polarization [50]. Blocking glycolysis suppressed TNFα production, but inhibiting citrate cycle enhanced TNFα production, which provided further evidence that anaerobic glycolysis polarized macrophages to M1 in pristane treated macrophages.

5. Conclusion

In conclusion, pristane stimulation damages mitochondria in macrophages, enhances anaerobic glycolysis of cells, leading to shifting of pro-inflammatory activation, which finally contributes to the development of arthritis (Fig. 7).

CRediT author statement

Xiaowei Li: Conceptualization, Data curation, Methodology, Project administration, Investigation, Visualization, Writing - original draft, Writing - review & editing. **Fengjie Gao:** Conceptualization, Methodology, Software, Writing - original draft, Writing - review & editing. **Wenhua Zhu:** Conceptualization, Methodology, Writing - original draft. **Congshan Jiang:** Data curation, Formal analysis. **Jing Xu:** Methodology, Validation. **Jing Zhang:** Validation, Resources. **Liesu Meng:** Conceptualization, Writing - review & editing. **Shemin Lu:** Conceptualization, Writing - review & editing.

Declaration of competing interest

The authors declare no conflict of interest.

Acknowledgement

The authors acknowledge Bioprofile Technology Co., Ltd. (Shanghai, China) for technical support on the quantitative proteomics analysis.

Appendix A. Supplementary data

Supplementary data to this article can be found online at https://doi.org/10.1016/j.yexcr.2020.112404.

Funding

This work is supported by the National Natural Science Foundation of China (81671629, 81970029 and 32070913), Shaanxi Province Natural Science Foundation, China (2020JQ082, 2018JM7057), the Fundamental Research Funds for the Central Universities, China (xjj2018159), and the Chunhui Program of Ministry of Education of China (2020).

References

[1] I.A. Udalova, A. Mantovani, M. Feldmann, Macrophage heterogeneity in the context of rheumatoid arthritis, Nat. Rev. Rheumatol. 12 (2016) 472–485.
[2] S. Solomon, N. Rajasekaran, E. Jeisy-Walder, S.B. Snapper, H. Illges, A crucial role for macrophages in the pathology of K/B x N serum-induced arthritis, Eur. J. Immunol. 35 (2005) 3064–3073.
[3] J. Li, H.C. Hsu, P. Yang, Q. Wu, H. Li, L.E. Edgington, M. Bogyo, R.P. Kimberly, J. D. Mountz, Treatment of arthritis by macrophage depletion and immunomodulation: testing an apoptosis-mediated therapy in a humanized death receptor mouse model, Arthritis Rheum. 64 (2012) 1098–1109.
[4] C.Q. Chu, M. Field, M. Feldmann, R.N. Maini, Localization of tumor necrosis factor alpha in synovial tissues and at the cartilage-pannus junction in patients with rheumatoid arthritis, Arthritis Rheum. 34 (1991) 1125–1132.
[5] R. Rueckert, K. Brandt, M. Ernst, K. Marienfeld, E. Csernok, C. Metzler, V. Budagian, E. Bulanova, R. Paus, S. Bulfone-Paus, Interleukin-15 stimulates macrophages to activate CD4(+) T cells: a role in the pathogenesis of rheumatoid arthritis? Immunology 126 (2009) 63–73.
[6] K.A. Gelderman, M. Hultqvist, A. Pizzolla, M. Zhao, K.S. Nandakumar, R. Mattsson, R. Holmdahl, Macrophages suppress T cell responses and arthritis development in mice by producing reactive oxygen species, J. Clin. Invest. 117 (2007) 3020–3028.
[7] W. Zhu, L. Meng, C. Jiang, J. Xu, B. Wang, Y. Han, S. Lu, Overexpression of toll-like receptor 3 in spleen is associated with experimental arthritis in rats, Scand. J. Immunol. 76 (2012) 263–270.
[8] L. Meng, X. He, W. Zhu, X. Yang, C. Jiang, Q. Sun, M. B, S. Zhang, Q. Xue, X. Xie, S. Lu, TLR3 and TLR7 modulate IgE production in antigen induced pulmonary inflammation via influencing IL-4 expression in immune organs, PloS One 6 (2011), e17252.
[9] L.A. O'Neill, R.J. Kishton, J. Rathmell, A guide to immunometabolism for immunologists, Nat. Rev. Immunol. 16 (2016) 553–565.
[10] L.A. O'Neill, E.J. Pearce, Immunometabolism governs dendritic cell and macrophage function, J. Exp. Med. 213 (2016) 15–23.
[11] C. Jing, T. Castro-Dopico, N. Richoz, Z.K. Tuong, J.R. Ferdinand, L.S.C. Lok, K. W. Loudon, G.D. Banham, R.J. Mathews, Z. Cader, S. Fitzpatrick, K.R. Bashant, M. J. Kaplan, A. Kaser, R.S. Johnson, M.P. Murphy, R.M. Siegel, M.R. Clatworthy, Macrophage metabolic reprogramming presents a therapeutic target in lupus nephritis, Proc. Natl. Acad. Sci. U. S. A. 117 (2020) 15160–15171.
[12] G.R. Bantug, L. Galluzzi, G. Kroemer, C. Hess, The spectrum of T cell metabolism in health and disease, Nat. Rev. Immunol. 18 (2018) 19–34.
[13] R. Bustos, F. Sobrino, Stimulation of glycolysis as an activation signal in rat peritoneal macrophages. Effect of glucocorticoids on this process, Biochem. J. 282 (Pt 1) (1992) 299–303.
[14] K.C. El Kasmi, K.R. Stenmark, Contribution of metabolic reprogramming to macrophage plasticity and function, Semin. Immunol. 27 (2015) 267–275.
[15] E.M. Palsson-McDermott, A.M. Curtis, G. Goel, M.A. Lauterbach, F.J. Sheedy, L. E. Gleeson, M.W. van den Bosch, S.R. Quinn, R. Domingo-Fernandez, D. G. Johnston, J.K. Jiang, W.J. Israelsen, J. Keane, C. Thomas, C. Clish, M. Vander Heiden, R.J. Xavier, L.A. O'Neill, Pyruvate kinase M2 regulates Hif-1alpha activity and IL-1beta induction and is a critical determinant of the warburg effect in LPS-activated macrophages, Cell Metabol. 21 (2015) 65–80.
[16] B. Kelly, L.A. O'Neill, Metabolic reprogramming in macrophages and dendritic cells in innate immunity, Cell Res. 25 (2015) 771–784.
[17] L.A. O'Neill, D.G. Hardie, Metabolism of inflammation limited by AMPK and pseudo-starvation, Nature 493 (2013) 346–355.
[18] J. Falconer, A.N. Murphy, S.P. Young, A.R. Clark, S. Tiziani, M. Guma, C. D. Buckley, Review: synovial cell metabolism and chronic inflammation in rheumatoid arthritis, Arthritis Rheum. 70 (2018) 984–999.
[19] S. Cohen, K. Danzaki, N.J. MacIver, Nutritional effects on T-cell immunometabolism, Eur. J. Immunol. 47 (2017) 225–235.
[20] W. Zhu, L. Meng, C. Jiang, X. He, W. Hou, P. Xu, H. Du, R. Holmdahl, S. Lu, Arthritis is associated with T-cell-induced upregulation of Toll-like receptor 3 on synovial fibroblasts, Arthritis Res. Ther. 13 (2011) R103.
[21] C. Vingsbo, P. Sahlstrand, J.G. Brun, R. Jonsson, T. Saxne, R. Holmdahl, Pristane-induced arthritis in rats: a new model for rheumatoid arthritis with a chronic disease course influenced by both major histocompatibility complex and non-major histocompatibility complex genes, Am. J. Pathol. 149 (1996) 1675–1683.
[22] M.G. Gutierrez, S.S. Master, S.B. Singh, G.A. Taylor, M.I. Colombo, V. Deretic, Autophagy is a defense mechanism inhibiting BCG and Mycobacterium tuberculosis survival in infected macrophages, Cell 119 (2004) 753–766.
[23] F. Wang, S. Zhang, I. Vuckovic, R. Jeon, A. Lerman, C.D. Folmes, P.P. Dzeja, J. Herrmann, Glycolytic stimulation is not a requirement for M2 macrophage differentiation, Cell Metabol. 28 (2018) 463–475 e464.
[24] W. Zhu, J. Xu, C. Jiang, B. Wang, M. Geng, X. Wu, N. Hussain, N. Gao, Y. Han, D. Li, X. Lan, Q. Ning, F. Zhang, R. Holmdahl, L. Meng, S. Lu, Pristane induces autophagy in macrophages, promoting a STAT1-IRF1-TLR3 pathway and arthritis, Clin. Immunol. 175 (2017) 56–68.
[25] L. Durnin, S.J. Hwang, M. Kurahashi, B.T. Drumm, S.M. Ward, K.C. Sasse, K. M. Sanders, V.N. Mutafova-Yambolieva, Uridine adenosine tetraphosphate is a novel neurogenic P2Y1 receptor activator in the gut, Proc. Natl. Acad. Sci. U. S. A. 111 (2014) 15821–15826.
[26] V.N. Mutafova-Yambolieva, S.J. Hwang, X. Hao, H. Chen, M.X. Zhu, J.D. Wood, S. M. Ward, K.M. Sanders, Beta-nicotinamide adenine dinucleotide is an inhibitory neurotransmitter in visceral smooth muscle, Proc. Natl. Acad. Sci. U. S. A. 104 (2007) 16359–16364.
[27] B.F. Howell, S. McCune, R. Schaffer, Lactate-to-pyruvate or pyruvate-to-lactate assay for lactate dehydrogenase: a re-examination, Clin. Chem. 25 (1979) 269–272.
[28] S. Summermatter, G. Santos, J. Perez-Schindler, C. Handschin, Skeletal muscle PGC-1alpha controls whole-body lactate homeostasis through estrogen-related receptor alpha-dependent activation of LDH B and repression of LDH A, Proc. Natl. Acad. Sci. U. S. A. 110 (2013) 8738–8743.
[29] A.M. Reynard, L.F. Hass, D.D. Jacobsen, P.D. Boyer, The correlation of reaction kinetics and substrate binding with the mechanism of pyruvate kinase, J. Biol. Chem. 236 (1961) 2277–2283.
[30] Q. Hua, C. Yang, T. Baba, H. Mori, K. Shimizu, Responses of the central metabolism in Escherichia coli to phosphoglucose isomerase and glucose-6-phosphate dehydrogenase knockouts, J. Bacteriol. 185 (2003) 7053–7067.
[31] G.E. Glock, L.P. Mc, Further studies on the properties and assay of glucose 6-phosphate dehydrogenase and 6-phosphogluconate dehydrogenase of rat liver, Biochem. J. 55 (1953) 400–408.
[32] J. Ding, J.E. Karp, A. Emadi, Elevated lactate dehydrogenase (LDH) can be a marker of immune suppression in cancer: interplay between hematologic and solid neoplastic clones and their microenvironments, Canc. Biomarkers 19 (2017) 353–363.
[33] J. Ho, M.B. de Moura, Y. Lin, G. Vincent, S. Thorne, L.M. Duncan, L. Hui-Min, J. M. Kirkwood, D. Becker, B. Van Houten, S.J. Moschos, Importance of glycolysis and oxidative phosphorylation in advanced melanoma, Mol. Canc. 11 (2012) 76.
[34] J. Tuncel, S. Haag, R. Holmdahl, MHC class II alleles associated with Th1 rather than Th17 type immunity drive the onset of early arthritis in a rat model of rheumatoid arthritis, Eur. J. Immunol. 47 (2017) 563–574.
[35] R. Holmdahl, J.C. Lorentzen, S. Lu, P. Olofsson, L. Wester, J. Holmberg, U. Pettersson, Arthritis induced in rats with nonimmunogenic adjuvants as models for rheumatoid arthritis, Immunol. Rev. 184 (2001) 184–202.
[36] F. Sakurai, T. Terada, K. Yasuda, F. Yamashita, Y. Takakura, M. Hashida, The role of tissue macrophages in the induction of proinflammatory cytokine production following intravenous injection of lipoplexes, Gene Ther. 9 (2002) 1120–1126.

[37] P.J. Murray, J.E. Allen, S.K. Biswas, E.A. Fisher, D.W. Gilroy, S. Goerdt, S. Gordon, J.A. Hamilton, L.B. Ivashkiv, T. Lawrence, M. Locati, A. Mantovani, F.O. Martinez, J.L. Mege, D.M. Mosser, G. Natoli, J.P. Saeij, J.L. Schultze, K.A. Shirey, A. Sica, J. Suttles, I. Udalova, J.A. van Ginderachter, S.N. Vogel, T.A. Wynn, Macrophage activation and polarization: nomenclature and experimental guidelines, Immunity 41 (2014) 14–20.

[38] R. Parsa, P. Andresen, A. Gillett, S. Mia, X.M. Zhang, S. Mayans, D. Holmberg, R. A. Harris, Adoptive transfer of immunomodulatory M2 macrophages prevents type 1 diabetes in NOD mice, Diabetes 61 (2012) 2881–2892.

[39] P.J. Murray, Macrophage polarization, Annu. Rev. Physiol. 79 (2017) 541–566.

[40] D. Xu, J. Liang, J. Lin, C. Yu, PKM2: a potential regulator of rheumatoid arthritis via glycolytic and non-glycolytic pathways, Front. Immunol. 10 (2019) 2919.

[41] F.A. van Gaalen, R.E. Toes, H.J. Ditzel, M. Schaller, F.C. Breedveld, C.L. Verweij, T. W. Huizinga, Association of autoantibodies to glucose-6-phosphate isomerase with extraarticular complications in rheumatoid arthritis, Arthritis Rheum. 50 (2004) 395–399.

[42] Y. Xiang, T. Sekine, H. Nakamura, S. Imajoh-Ohmi, H. Fukuda, K. Nishioka, T. Kato, Proteomic surveillance of autoimmunity in osteoarthritis: identification of triosephosphate isomerase as an autoantigen in patients with osteoarthritis, Arthritis Rheum. 50 (2004) 1511–1521.

[43] D.C. Fuhrmann, B. Brune, Mitochondrial composition and function under the control of hypoxia, Redox Biol 12 (2017) 208–215.

[44] E.K. Kim, J.E. Kwon, S.Y. Lee, E.J. Lee, D.S. Kim, S.J. Moon, J. Lee, S.K. Kwok, S. H. Park, M.L. Cho, IL-17-mediated mitochondrial dysfunction impairs apoptosis in rheumatoid arthritis synovial fibroblasts through activation of autophagy, Cell Death Dis. 8 (2017) e2565.

[45] R. Garcia-Carbonell, A.S. Divakaruni, A. Lodi, I. Vicente-Suarez, A. Saha, H. Cheroutre, G.R. Boss, S. Tiziani, A.N. Murphy, M. Guma, Critical role of glucose metabolism in rheumatoid arthritis fibroblast-like synoviocytes, Arthritis Rheum. 68 (2016) 1614–1626.

[46] J. Van den Bossche, L.A. O'Neill, D. Menon, Macrophage immunometabolism: where are we (going)? Trends Immunol. 38 (2017) 395–406.

[47] L.A. O'Neill, E.J. Pearce, Immunometabolism governs dendritic cell and macrophage function, J. Exp. Med. (2015).

[48] A.K. Jha, S.C. Huang, A. Sergushichev, V. Lampropoulou, Y. Ivanova, E. Loginicheva, K. Chmielewski, K.M. Stewart, J. Ashall, B. Everts, E.J. Pearce, E. M. Driggers, M.N. Artyomov, Network integration of parallel metabolic and transcriptional data reveals metabolic modules that regulate macrophage polarization, Immunity 42 (2015) 419–430.

[49] G. Chen, Z.D. Cai, Z.Y. Lin, C. Wang, Y.X. Liang, Z.D. Han, H.C. He, R.J. Mo, J. M. Lu, B. Pan, C.L. Wu, F. Wang, W.D. Zhong, ARNT-dependent CCR8 reprogrammed LDH isoform expression correlates with poor clinical outcomes of prostate cancer, Mol. Carcinog. 59 (2020) 897–907.

[50] C. Loh, S.H. Park, A. Lee, R. Yuan, L.B. Ivashkiv, G.D. Kalliolias, TNF-induced inflammatory genes escape repression in fibroblast-like synoviocytes: transcriptomic and epigenomic analysis, Ann. Rheum. Dis. 78 (2019) 1205–1214.